national accelerator laboratory

NAL-Pub-73/53-EXP
2257.000

Yale-3075-49

(Submitted to Nucl. Instr. and Methods)

THE DESIGN AND OPERATION OF THE YALE-NAL-BNL HYPERON BEAM

V. Hungerbuehler, H. Kraybill, R. Majka, J. N. Marx,
P. Némethy, J. Sandweiss, W. Tanenbaum,
W. J. Willis, and I. J. Winters
Yale University, New Haven, Connecticut 06520 USA

M. Atac, S. Ecklund, P. J. Gollon, J. Lach, J. MacLachlan,
A. Roberts, R. Stefanski, and D. Theriot
National Accelerator Laboratory, Batavia, Illinois 60510 USA

and

C. L. Wang
Brookhaven National Laboratory, Upton, New York 11973 USA

August 1973

NAL-Pub-73/53-EXP

THE DESIGN AND OPERATION OF THE YALE-NAL-BNL HYPERON BEAM

V. Hungerbuehler, H. Kraybill, R. Majka, J. N. Marx,
P. Némethy, J. Sandweiss, W. Tanenbaum,
W. J. Willis, and I. J. Winters
Yale University, New Haven, Connecticut 06520 USA*

M. Atac, S. Ecklund, P. J. Gollon, J. Lach, J. MacLachlan,
A. Roberts, R. Stefanski, and D. Theriot
National Accelerator Laboratory, Batavia, Illinois 60510 USA

and

C. L. Wang
Brookhaven National Laboratory, Upton, New York 11973 USA†

ABSTRACT

The design and operation of a negative hyperon beam is described. Fluxes of 200 Σ^- and 2 Ξ^- per 1.5×10^{11} interacting protons are delivered to a double magnetic spectrometer where decay products are analyzed. Hyperons are identified by kinematic fitting of their decays.

I. INTRODUCTION

The use of electronic detectors to study the properties of hyperons with good statistical accuracy has been a goal of high-energy physicists for almost a decade. Until recently, however, electronic techniques have not supplanted the bubble chamber as the primary tool for studying these short-lived particles (lifetime $\sim10^{-10}$ sec) because no high-intensity source has been available. In this paper we report on the design, construction, and operation of a high-energy negative hyperon beam and its associated electronic detection

system. The beam and detector have successfully been used for several experiments, including studies of hyperon production,[1] leptonic decays,[2] isobar production,[3] and elastic scattering.[4]

A high-energy hyperon beam is essentially a magnetic channel designed to transport the desired particles from their point of production to the detection apparatus. The beam components must also shield the detector from undesired background radiation, define the momentum of the beam particles, and, ideally, identify beam hyperons before they decay or interact or at least provide a veto for less massive unwanted beam particles. The short lifetime of the hyperons provides a severe constraint in the design of the beam--a useful fraction of the particles must reach the detection apparatus before they decay. For this reason, the hyperons must be produced with as high an energy as possible so as to maximize the time dilation effect, and the beam must be as short as possible consistent with shielding requirements. As an additional benefit, the production kinematics are such that as the secondary particle momentum is increased, the hyperon-to-meson ratio increases.[1] In order to meet these requirements at accelerators, one needs a slowly extracted proton beam so that the secondary-beam channel can capture hyperons produced in the forward direction and bring them into an accessible low-background region in the short distance available. The construction of hyperon beams thus had to await the development of useful slowly extracted proton beams.

II. THE HYPERON BEAM

The slowly extracted proton beam[5] at the Brookhaven National Laboratory Alternating Gradient Synchrotron (AGS) provides 3×10^{11} protons of momentum 29.4 GeV/c per machine pulse at the C' external target station.

The beam size is typically 0.25 in. in diameter. Figure 1 illustrates the arrangement for targeting the proton beam and the subsequent hyperon beam and detector. Hyperons are produced in a $0.23 \times 0.23 \times 10$ in. beryllium target located at the entrance to a pair of 18D72 magnets. The magnet gaps were reduced to 1 in. using a cobalt-steel alloy so that fields of over 32 kG could be obtained. A 21-in. tungsten plug located 24 in. downstream from the target acted as a beam dump. Beginning 24 in. downstream from the first magnet entrance the magnet gaps were filled with brass which served as a hadron shield for the detectors. A tapered channel of radius 1000 in. was cut in the brass. This channel is 0.25 in. wide and 0.50 in. high from the beam dump to the end of the first magnet. Following a 12-in. long straight section in the field free region between magnets, the channel tapers to 0.75 in. wide by 0.875 in. high at the end of the second magnet. Primary protons which have not interacted in the target or which have quasi-elastically scattered are bent away from the channel into the beam dump. Negative particles produced in the desired solid angle and momentum bite are transported by the channel to the detectors located after the magnets. The channel has a solid angle acceptance of 22 μsr and a momentum acceptance of approximately 10% (FWHM). The total path length from the target to the channel exit is 172 in. with a 8.4° bend.

In the design of the magnetic channel, careful consideration was given to the problem of muons produced by pions which decay before being absorbed in the beam dump. These muons are generally of lower momentum than those accepted by the channel. They are deflected away from the channel by the

magnetic field. However, near the return yokes the magnetic field changes direction, and the lower energy muons are deflected back towards the channel. This effect results in muons oscillating between the main field and the return yokes as they travel downstream through the channel magnets. A muon of a given momentum and initial direction oscillates with a characteristic phase which determines its direction after it leaves the downstream face of the second channel magnet. A careful Monte-Carlo study[6] was made to calculate the size and direction of the beams of muons which emerge from the magnets on either side of the channel opening. The geometry was arranged so that these muons are directed away from the detectors. The idea of using superconducting dipoles as channel magnets was rejected because the return legs would have been too close to the beam line. Such a design would have produced excessive muon fluxes through the detectors.

The second half of the channel also acted as a threshold Cerenkov counter. Aluminized epoxy-coated brass inserts made the internal channel walls reflective. Gas-tight mylar windows covered the channel openings between the magnets and at the channel exit; this volume was filled with Freon 13B1 gas.[7] A 5 μm thick pellicle mirror at the channel exit tilted 45° to the beam directed light to a 56DVP photomultiplier tube. The inefficiency of the device for pions has been measured to be less than 10^{-3}. A Monte-Carlo simulation of the collection of light from this detector predicted a minimum of 60 photons reaching the phototube. The index of refraction of Freon 13B1 at atmospheric pressure is such that this beam Cerenkov counter (C_B) is sensitive to particles of mass less than about 1 GeV. As a result we

can tag unwanted beam pions, kaons, and electrons with high efficiency. A scintillation counter (V_π) placed at the downstream end of the detector provided an additional veto for stable beam particles.

A high pressure, high-resolution spark chamber is located immediately following the channel exit. This chamber has been described in detail elsewhere.[8] It operates at 10 atmospheres and gives a spatial resolution of less than 100 μm. The cluster used in the hyperon beam measures eight coordinates (X, Y, U, X, Y, V, X, Y)[9] and determines the hyperon direction to better than 0.5 mrad with a minimal decay loss. Assuming a point production target, the momentum of beam particles can be determined to better than ±1%. The high resolution chamber was sandwiched between small beam defining trigger counters (B).

The short-lived particle beam described above transmits Σ^- and Ξ^- hyperons to the decay region with a decay loss of 99.4% at 23 GeV/c. Muons from the beam dump are directed away from the detectors. Unwanted light beam particles are tagged in a fashion suitable for use as a veto in a fast electronic trigger. The momentum and direction of the emerging hyperons are determined to ±1% and better than 0.5 mrad respectively.

III. DETECTORS AND HYPERON IDENTIFICATION

The detection apparatus described below was designed to identify hyperons by their predominant two-body decay modes. Variants of the apparatus used to study leptonic decays, isobar production, and elastic scattering are described elsewhere.[6,10,11]

The apparatus is sensitive to $n\pi^-$ final states from Σ^- decay and $\Lambda^o\pi^-$ (Λ^oK^-) final states from Ξ^- (Ω^-) decay. The final state lambdas are observed through their decays to π^-p. In each case the final state consists of either a neutron and a single relatively low momentum negative meson or, when a lambda is present, a proton and two negative mesons. The detection apparatus was designed to identify neutrons, protons, and slow negative particles and to trigger on the appropriate combinations.

The detection apparatus is also shown in Fig. 1. Following the high resolution spark chamber is a 115-in. long decay region and two conventional magnetic spectrometers. Each magnet has a 10-in. gap and is excited to approximately 13 kG. The spark chambers located on either side of the magnets have 0.5-mm wire spacing with magnetostrictive readout. Each cluster consists of five planes so that ten coordinates (3X, 3Y, 2U, 2V)[9] are measured at the entrance and exit of each spectrometer magnet. The first magnet is used to momentum-analyze the slow negative decay products while the second analyzes the fast protons from lambdas. A scintillation counter hodoscope (S) is located between the magnets and is used to trigger on slow negative decay products.

Following the second spectrometer magnet is the apparatus to identify high momentum (~15 GeV/c) neutrons and protons. The proton detector consists of a cluster of magnetostrictive chambers and trigger counters (P) to determine the proton position after the second spectrometer magnet. This cluster is followed by a calorimeter (PC) consisting of iron and scintillator sandwiches. This calorimeter is required to produce sufficient pulse height

to assure the presence of a hadron thus rejecting background muons which could otherwise trigger the detectors.

The neutron detector consists of a set of 5 modules,[12] each consisting of a 1.25-in. iron plate, an XY multiwire proportional chamber with 1 cm wire spacing, and a scintillation counter. The total amount of material in the detector is 1.5 interaction lengths. The neutron interaction point can be determined to about 1 cm transverse to the beam direction by studying the development of the resulting hadron shower in these modules.[13] The large lever arm between the decay vertex and the neutron detector gives a measurement of the neutron angle to 1 mrad. The neutron detector also contains a neutron calorimeter (NC). In order to discriminate against muons, the neutron trigger requires a minimum pulse height from this calorimeter.

IV. DETECTOR OPERATION AND RESULTS

Two different triggers were used to study the beam fluxes of Σ^- and Ξ^- respectively. The Σ^- trigger was (see Fig. 1)

$$\Sigma^- = \bar{C}_B \cdot B \cdot S \cdot NC \cdot \bar{V}_\pi ,$$

that is, a massive beam particle below threshold in the beam Cerenkov counter, a slow negative particle after the first magnetic spectrometer, a high-energy neutron and nothing striking the downstream beam scintillation counter veto. The Ξ^- trigger was

$$\Xi^- = \bar{C}_B \cdot B \cdot S \cdot P \cdot PC \cdot \bar{V}_\pi ,$$

where in this case a high-energy proton rather than a neutron was required. In addition, the apparatus was triggered on a small fraction of the beam pions to provide a convenient normalization and a monitor of the spark-chamber

efficiency. Periodically, the spectrometer magnets were turned off and the beam pions were used to align the spark chambers. For an incident interacting intensity of approximately 1.5×10^{11} protons per AGS pulse, the flux emerging from the hyperon channel was about 30,000 π^-, 200 Σ^-, and 2 Ξ^- at a channel central momentum of 23 GeV/c.

The requirement of a massive beam particle and a high-energy neutral or positively charged hadron downstream from the decay region provided a very clean trigger. Background muons, which can snake through the magnetic fields in the beam and spectrometers and so strike the various trigger counters, were effectively eliminated by the hadron calorimeters. Figure 2 depicts a pulse height spectrum from the neutron calorimeter using incident pions of momentum greater than 20 GeV/c. The low-energy tail represents muon contamination. This figure illustrates the effectiveness of this calorimeter with an appropriate pulse height requirement for the rejection of muons.

In order to measure the hyperon fluxes in the beam, the triggered events were reconstructed with the appropriate two-body hypothesis. For this hypothesis the information on the neutron interaction point was not used for the Σ^- triggers. These events are then once overconstrained so that the incident beam particle mass can be calculated. The resulting mass spectrum is shown in Fig. 3. The only cuts made in obtaining this mass plot were fiducial volume cuts, channel phase space cuts to assure that the beam particle came from the production target, a decay vertex cut, and a minimum decay angle requirement of 5 mrad to allow the decay point to be accurately defined. About 50% of the $\Sigma^- \rightarrow n\pi^-$ triggers passed these cuts. No kinematic

cuts were made. The mass plot indicates an essentially pure Σ^- signal with a resolution of ~10 MeV.

Events from the Ξ^- trigger were reconstructed in a two-step process. First a fit was made to the hypothesis $\Lambda^o \rightarrow \pi^- p$ and then to the hypothesis $\Xi^- \rightarrow \Lambda^o \pi^-$ thus giving a four-constraint fit. Spatial cuts, similar to those used for the Σ^- triggers were also imposed. About 5% of the $\Xi^- \rightarrow \Lambda^o \pi^-$ triggers passed these cuts and were reconstructable. Losses resulted from upstream decays, the extra decay length required for the Λ^o, and the smaller solid angle for the detection of the decay proton. The resulting mass spectrum is shown in Fig. 4. Here again the hyperon signal is essentially pure with a mass resolution of ~2 MeV.

The Yale-NAL-BNL hyperon beam has shown its capabilities for providing large fluxes of high-energy negative hyperons. The associated detection apparatus allows the experimenter to select a series of triggers which result in a pure sample of reconstructed events which have been used to study the production and decay properties of hyperons.[1-4]

ACKNOWLEDGMENTS

We wish to thank our engineering staff, Satish Dhawan, Cordon Kerns, and Blaise Lombardi, and our technicians Jon Blomquist, Ed Steigmeyer, and Alan Wandersee for their help in the design and setup of the apparatus. Carl Dolnick aided in programming the online computer. We thank the University of Michigan group and the University of Pittsburgh group for the

use of their scintillation counter calorimeters. We also thank the AGS staff, in particular David Berley, for providing the technical support needed for the success of this program.

FOOTNOTES AND REFERENCES

*Research supported by the United States Atomic Energy Commission under Contract AT(11-1).

†Supported by the United States Atomic Energy Commission.

[1] S. Ecklund et al., Bull. Am. Phys. Soc. 18, 693 (1973); V. Hungerbuehler et al., Phys. Rev. Letters 24, 1234 (1973).

[2] W. Tanenbaum et al., Bull. Am. Phys. Soc. 18, 616 (1973).

[3] C. Wang et al., Bull. Am. Phys. Soc. 18, 694 (1973).

[4] R. Majka et al., Bull. Am. Phys. Soc. 18, 694 (1973).

[5] L. N. Blumberg, Slow External Beam - Performance and Plans, Brookhaven National Laboratory Summer Study on AGS Utilization 1970, BNL-16000.

[6] W. J. Willis et al., AGS Proposal 430 (unpublished).

[7] The chemical composition of Freon 13B1 is $CBrF_3$.

[8] W. J. Willis et al., Nucl. Instr. and Methods 91, 33 (1971).

[9] U and V coordinates are rotated by 45° with respect to vertical (X) and horizontal (Y) coordinates.

[10] J. N. Marx et al., AGS Proposal 571 (unpublished).

[11] J. N. Marx et al., AGS Proposal 573 (unpublished).

[12] M. Atac et al., Nucl. Instr. and Methods 106, 263 (1973).

[13] W. Tanenbaum, Nucl. Instr. and Methods 106, 269 (1973).

FIGURE CAPTIONS

Fig. 1. Schematic diagram of the high-energy hyperon beam at the BNL AGS.

Fig. 2. Typical pulse height spectrum from the neutron calorimeter.

Fig. 3. Typical Σ^- reconstructed mass spectrum.

Fig. 4. Typical Ξ^- reconstructed mass spectrum.

HIGH ENERGY NEGATIVE HYPERON BEAM

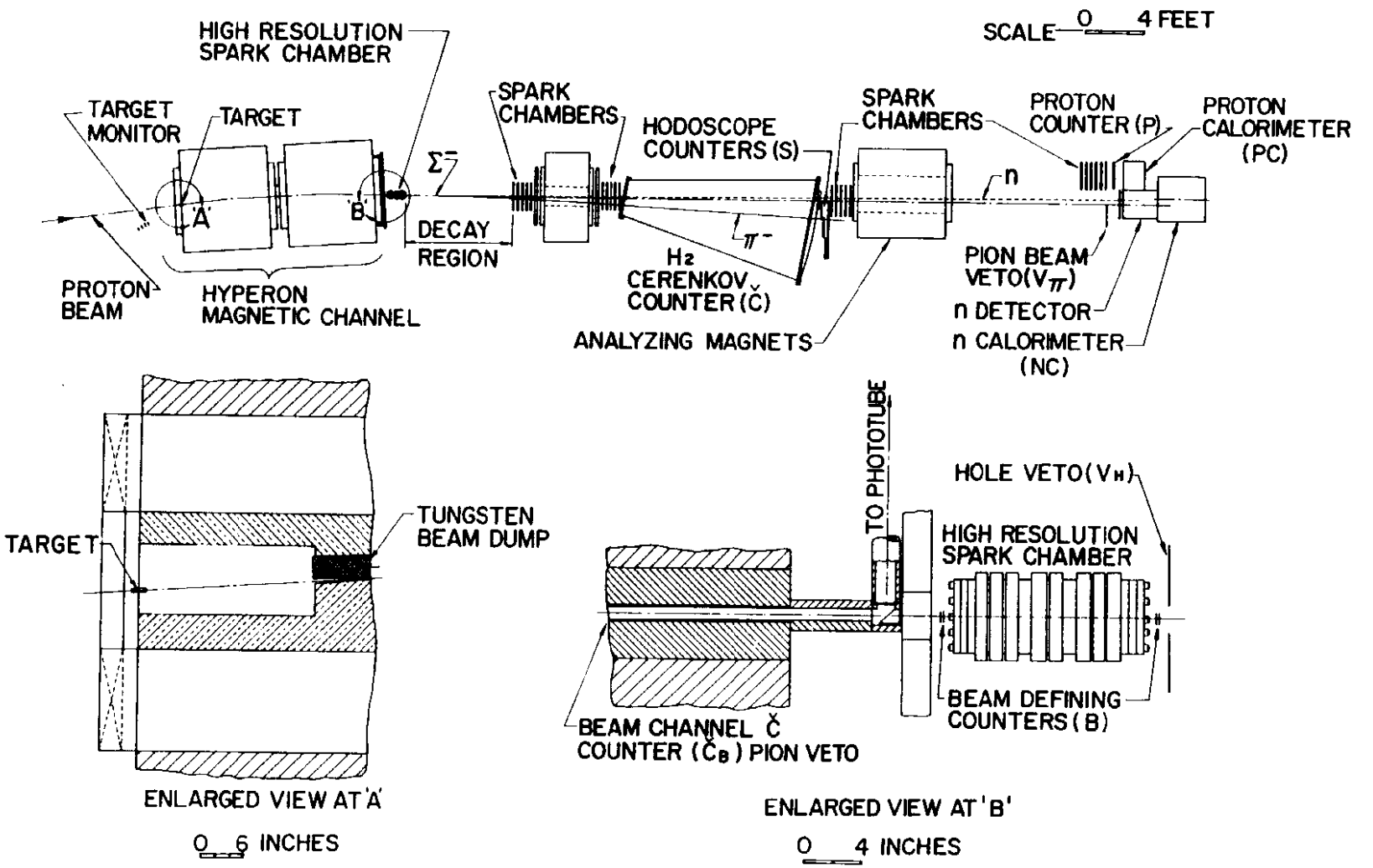

Fig. 1

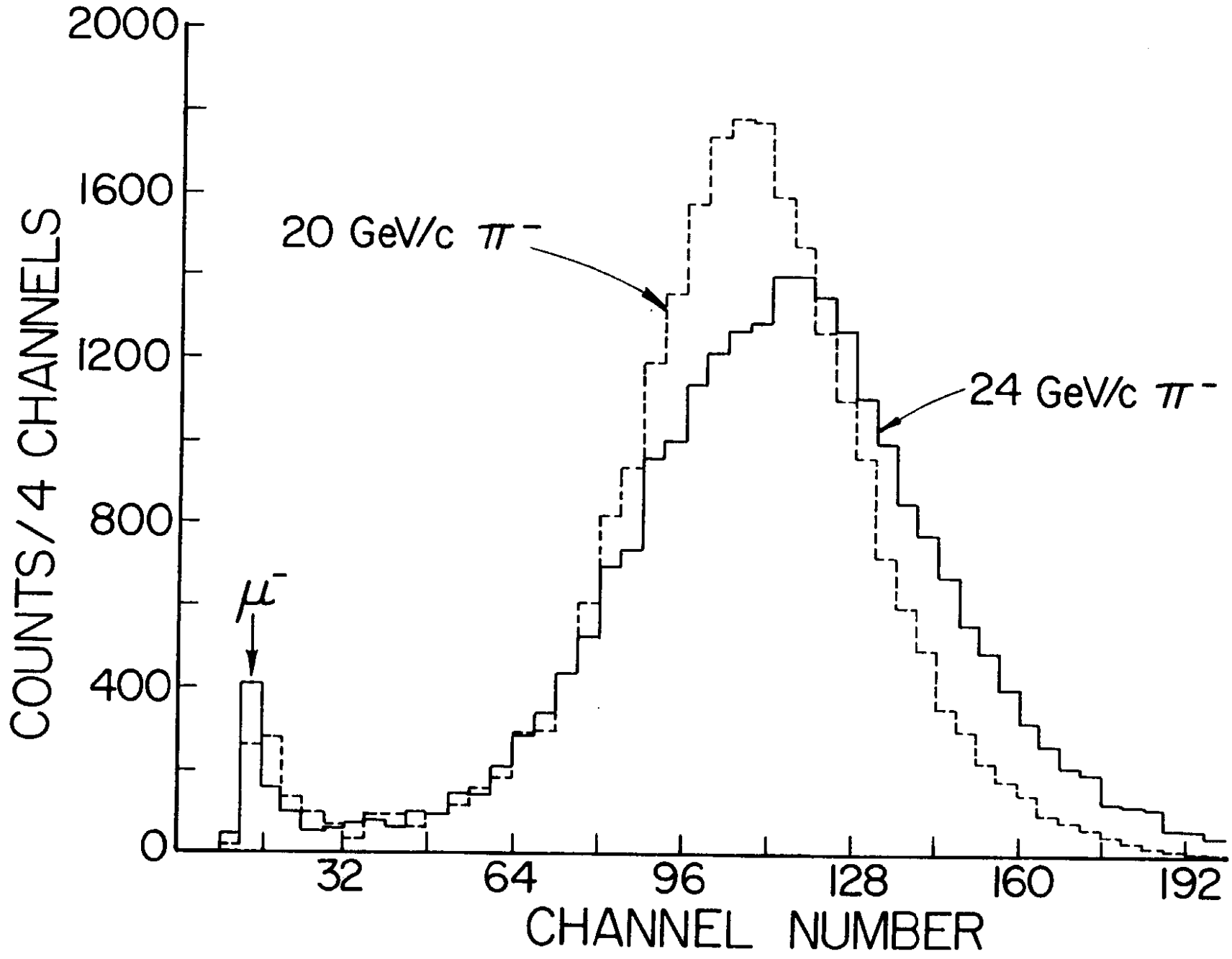
2000
1600
1200
800
400
0
COUNTS/4 CHANNELS
20 GeV/c π⁻
24 GeV/c π⁻
μ⁻
32
64
96
128
160
192
CHANNEL NUMBER

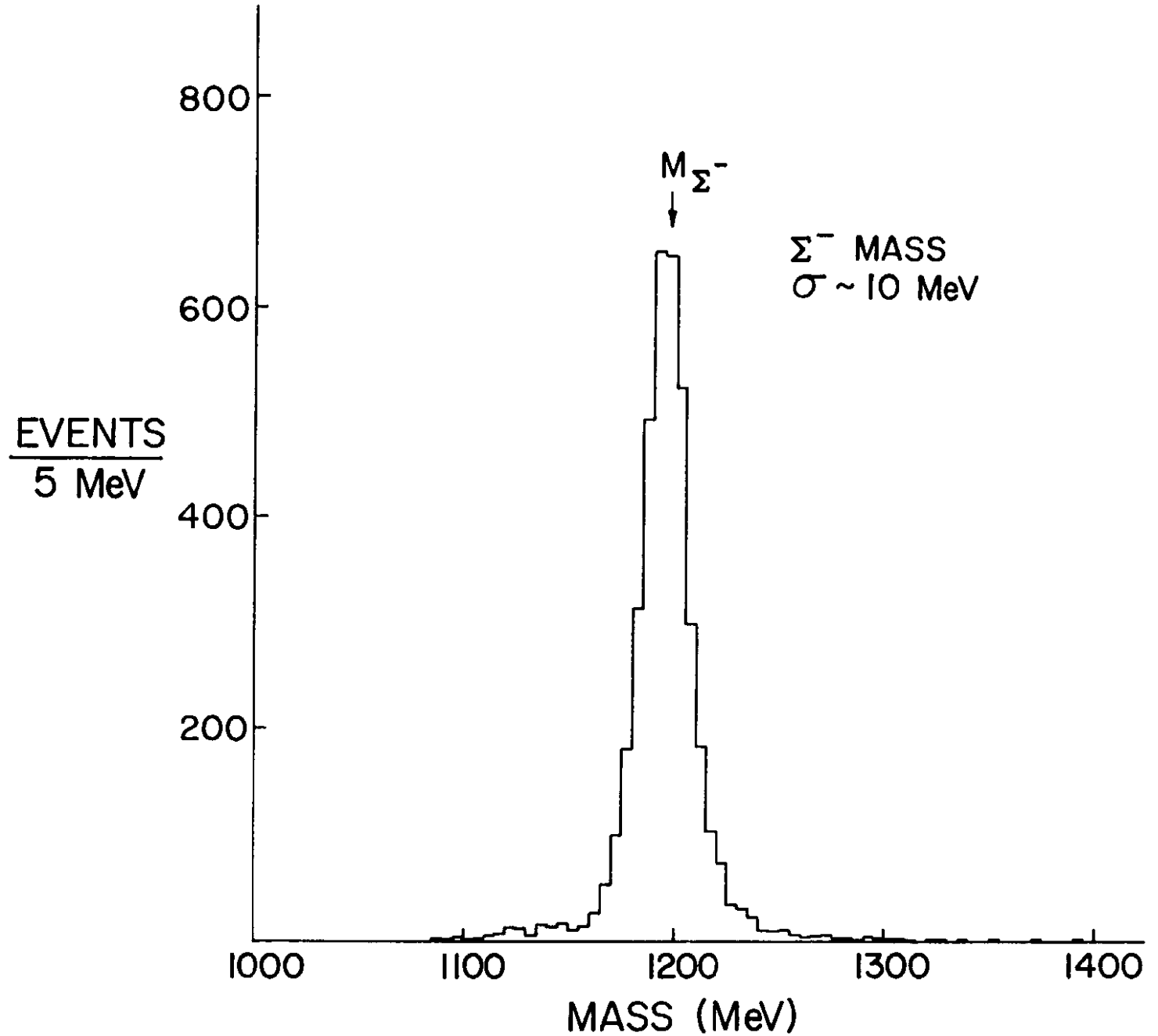
800
600
400
200
EVENTS
5 MeV
M_{Σ^-}
Σ^- MASS
$\sigma \sim 10$ MeV
1000
1100
1200
1300
1400
MASS (MeV)

Fig. 3

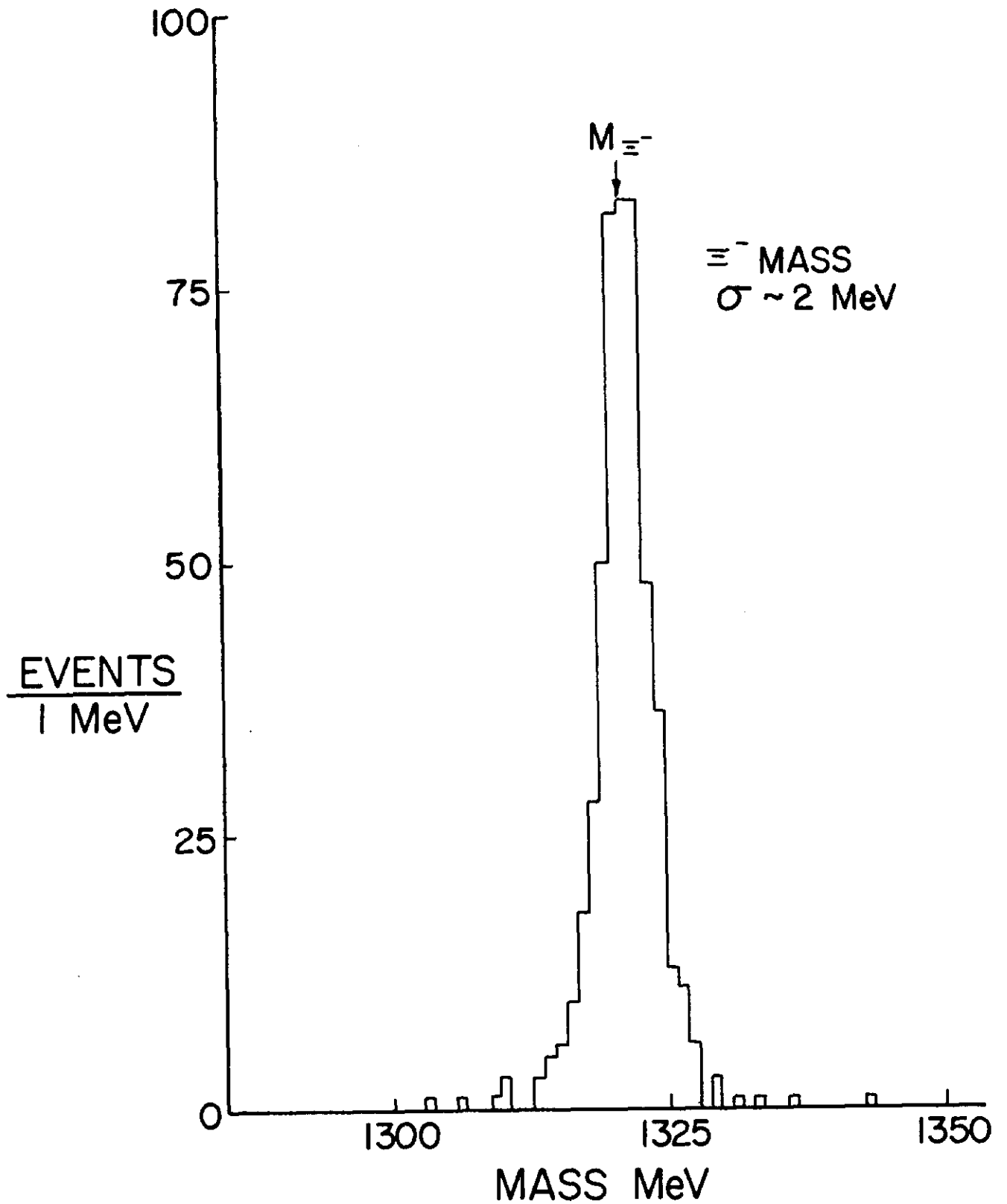
100
75
50
25
0
EVENTS
1 MeV
M Ξ⁻
Ξ⁻ MASS
σ ~ 2 MeV
1300
1325
1350
MASS MeV

Fig. 4